Available on CMS information server

CMS NOTE 2004/032

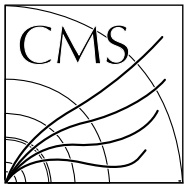

The Compact Muon Solenoid Experiment

CMS Note

Mailing address: CMS CERN, CH-1211 GENEVA 23, Switzerland

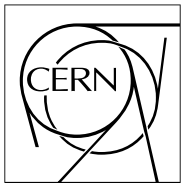

June, 2004

Validation of GEANT4 Physics Using 1996 CMS HCAL Test Beam Data

Sudeshna Banerjee[a)], Sunanda Banerjee[a,b)]

Abstract

Various hadronic physics models of GEANT4 are validated for the first time using the 1996 test beam data of the CMS hadron calorimeter. Detailed comparison have been carried out on energy response, energy resolution and longitudinal shower profiles between the test beam data with electron and pion beams at different energies and simulation of the associated setup with different models in GEANT4 and GEANT3. Gross features in the data, like non-linearity in energy response, energy resolution, etc. are well reproduced by the Monte Carlo models. There are some disagreements in some of the details like longitudinal shower profiles or the e/h ratio.

[a)] Tata Institute of Fundamental Research, Mumbai

[b)] PH Division, CERN

1 Introduction

High energy experiments depend critically on the accuracy of the description of the behaviour of the detector to passage of particles of known energies. This is achieved using simulation programmes describing electromagnetic as well as hadronic processes. An accurate description of hadronic interactions and hadronic showers over a broad energy range is the most challenging part of any package which will be used to simulate the environment of an experiment at the Large Hadron Collider (LHC).

Simulated data are used to optimise the detector design, to understand how the detector performs and what the reconstruction or analysis software does to the data corresponding to a given physics process. So the ultimate systematic uncertainties of a given measurement from an experiment is strongly related to the accuracy of simulation of detector performance.

The Compact Muon Solenoid (CMS) experiment [1] at the LHC will use GEANT4 [2] toolkit to simulate its performance. The CMS detector consists of an electromagnetic calorimeter and a hadronic part. The electromagnetic calorimeter (ECAL) consists of $PbWO_4$ crystals arranged in towers. The hadron calorimeter (HCAL) is of the sampling kind. It is a sandwich of scintillator plates with brass absorber in-between. The total absorber thickness amounts to approximately 11 interaction lengths over a large η range. Light is collected from scintillator using green Wave Length Shifting (WLS) fibres. This light is then transmitted to the readout electronics through clear fibres of low attenuation length.

A mockup of this calorimeter was made and tested [3] in a particle beam in 1996. This mockup geometry has been simulated using GEANT4 [2] and GEANT3 [4]. The data have been analysed in the same way as data from the test beam experiment.

The features that are compared here are

- energy deposits in individual scintillator layers.
- longitudinal shower development.
- effect of the contribution from the electromagnetic calorimeter (e/π effects).
- changes in the above features in the presence of a magnetic field.

2 1996 Test Beam Setup for CMS HCAL

The test beam prototype of HCAL is based on a hanging file structure, in which absorber plates made out of a special type of brass (composed of 59% copper, 39% zinc, 1% iron, 1% manganese by weight) and varying in thickness from 2 cm to 8 cm are sandwiched with scintillator tiles. There are 28 tiles, mostly 4 mm thick. Figure 1 shows the layout of the hanging file structure. The tiles are read out with WLS fibres connected to photomultiplier. For a detailed description of the 1996 test beam setup and data analysis, refer to [3].

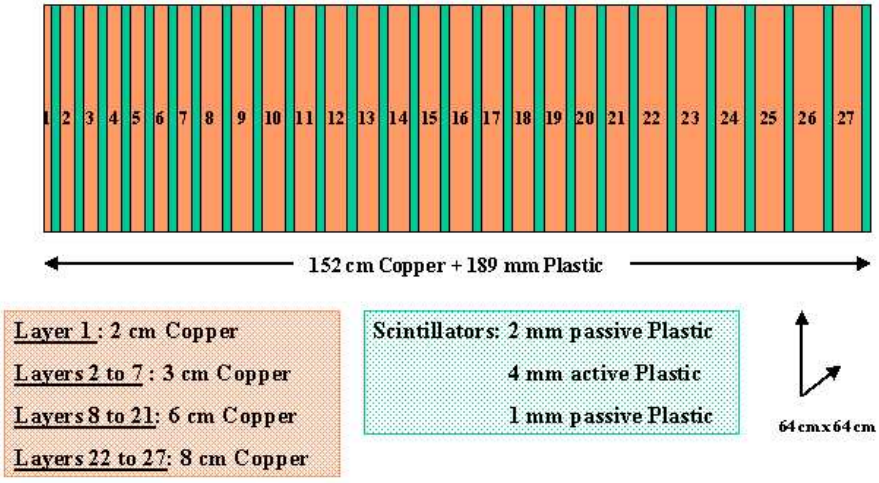

Figure 1: A schematic view of the 1996 CMS HCAL Test Beam Setup.

The hanging file structure of HCAL was preceded (part of the time) with an ECAL module consisting of 49 lead tungstate crystals arranged in the form of a 7×7 matrix. Each crystal was 23 cm long and of size 20.5×20.5 cm^2 in the front face and 23.8×23.8 cm^2 in the rear. The total radiation length is 25.8 and the interaction length is 1.1. The crystals are read out individually using APD's with approximate gain of 50.

During the 1996 test beam, data were recorded with several different particle beams going through the HCAL mockup detector. Beams and their energies were as follows:

- electron beam with energies 10, 15, 20, 30, 50, 100, 150, 300 GeV.
- pion beam with energies 10, 15, 20, 30, 50, 100, 150, 300 GeV.
- muon beam with 225 GeV energy.

One set of data were taken with only HCAL in the beam. Another set was taken with ECAL upstream of HCAL in the beam. Electron and pion beams were used to calibrate ECAL and HCAL respectively and also to study the response (ratio of measured energy and actual beam energy) of ECAL and HCAL due to the passage of electrons and pions. Muon beams were used to normalise the response of the different HCAL scintillator layers. More than 10000 events were collected for each particle and each energy.

All the test beam data taken with HCAL only and ECAL+HCAL system were repeated in the presence of a solenoidal magnetic field. The strength of the magnetic field could be increased up to 3 Tesla. Data were taken in several steps from 0 to 3 Tesla. The field direction was parallel to the face of the scintillator tiles which simulates the HCAL barrel in the CMS experiment. The field was not uniform over all of ECAL and HCAL. Figure 2 gives a map of the magnetic field covering the positions of ECAL and HCAL in the test beam.

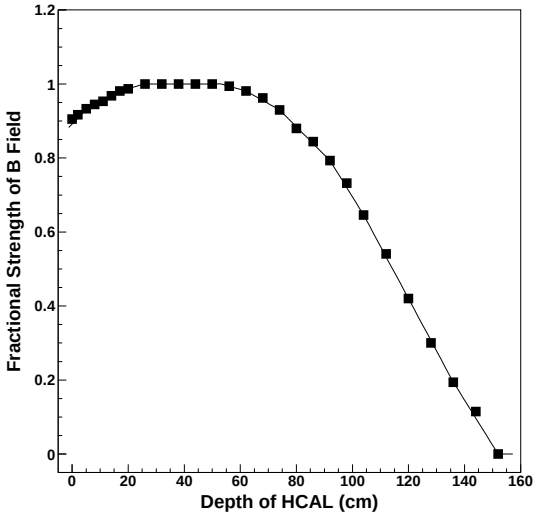

Figure 2: Relative strength of the magnetic field as a function of depth in HCAL (from the front face) as in test beam 1996.

3 Simulation of Test Beam Setup

GEANT4 version 4-05-02-patch-02 has been used to simulate the test beam geometry. The geometry of the two calorimeter modules are described in detail but the beam line components are left out in the simulation. A cutoff of 700 μm is used on the range of particles in all the materials. The following four physics lists with the PACK 2.3 version of the packaging system are used for the hadronic physics.

- LHEP (parametrised models for inelastic scattering)
- QGSP (a quark gluon string model and a pre-equilibrium decay model with an evaporation phase to model the behaviour of the nucleus)

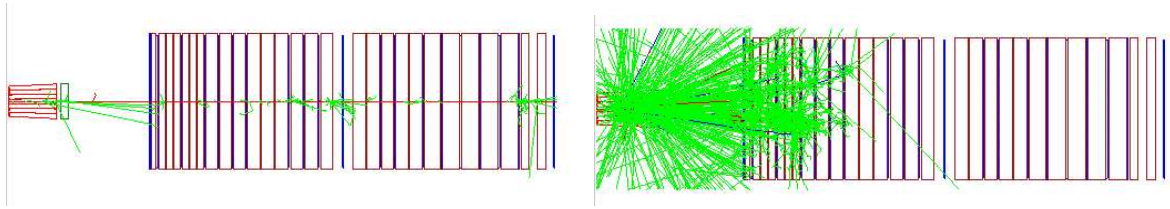

Figure 3: A view of the simulated 1996 CMS HCAL Test Beam Setup in the GEANT4 framework: (a) due to passage of a muon, (b) due to passage of a hadron.

- QGSC (QGSP for the initial reaction and with a chiral invariant phase-space decay)
- FTFP (diffractive string excitation model similar to that in Fritjof and the Lund fragmentation functions)

Figure 3 shows the passage of a muon and that of a hadron through the ECAL+HCAL system. For setup with magnetic field, the proper field map as shown in Figure 2 was implemented. The classical Runge Kutta field integrator is used with precision values for stepping, intersection and chord finding set at small values (~ 1 μm).

For ECAL, a correction is made for the small inhomogeneity in light collection in the crystals along their length. Electronic noise in the Calorimeter readout is simulated by studying the width of energy distribution in each HCAL layer and ECAL tower using random triggers (pedestal events). Figures 4 and 5 show examples of the noise distribution. This noise is added to the energy simulation for each channel in HCAL and ECAL.

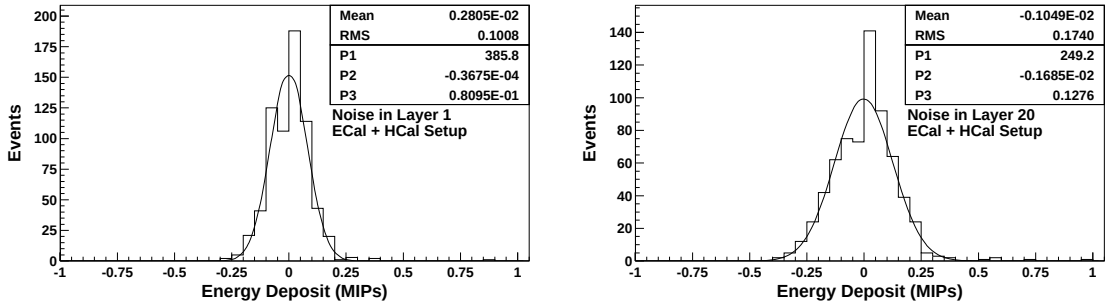

Figure 4: Energy measurement in HCAL layers 1 and 20 with random trigger in the 1996 test beam data.

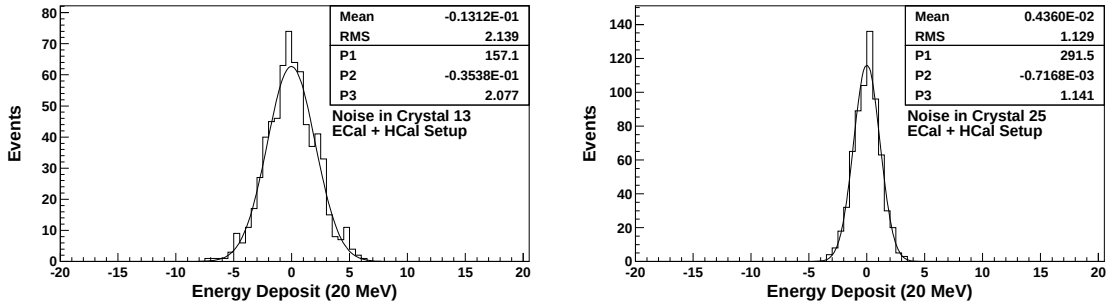

Figure 5: Energy measurement in ECAL towers 13 and 25 with random trigger in the 1996 test beam data.

Events are also generated using the GEANT 3.21 package with the GHEISHA package simulating the hadron showers. A 100 KeV cutoff is used for photon, electron and charged hadrons and a 10 KeV cutoff is used for neutrons. Incorporation of the magnetic field and handling of electronic noise and non-uniformity of crystals are done in the same way as in the case of GEANT4.

Event samples of typical size between 5000 to 20000 are generated for each setup. Test beam data are compared to simulation results obtained with each physics list of GEANT4 and also with GEANT3 [4].

4 Data Analysis Procedure

4.1 Normalisation with Muons

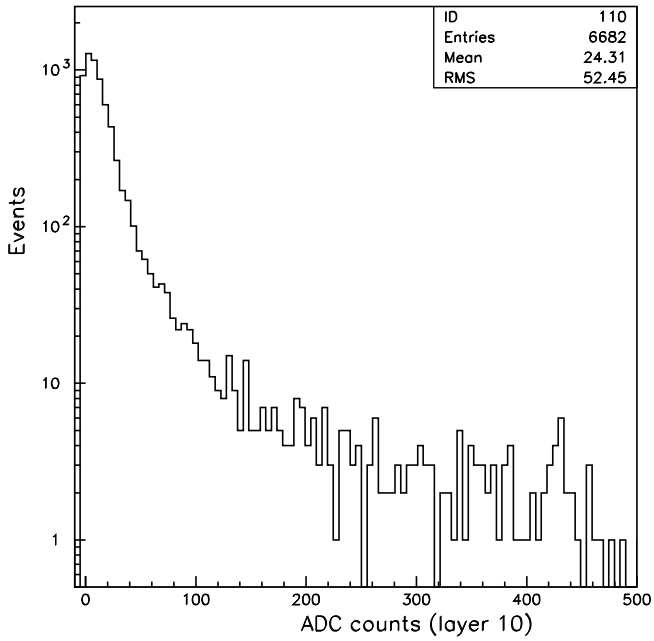

Figure 6: Energy deposit in HCAL layer 10 with 225 GeV muon beam in the test beam data (ADC counts).

A relative calibration of the scintillator layers is done by comparing the response of the layers to a 225 GeV muon beam. Figure 6 shows the ADC distribution for scintillator layer 10 from test beam data. The mean of the distribution is taken as the calibration constant for that particular layer. The accuracy of this measurement is of the order of 3% [3].

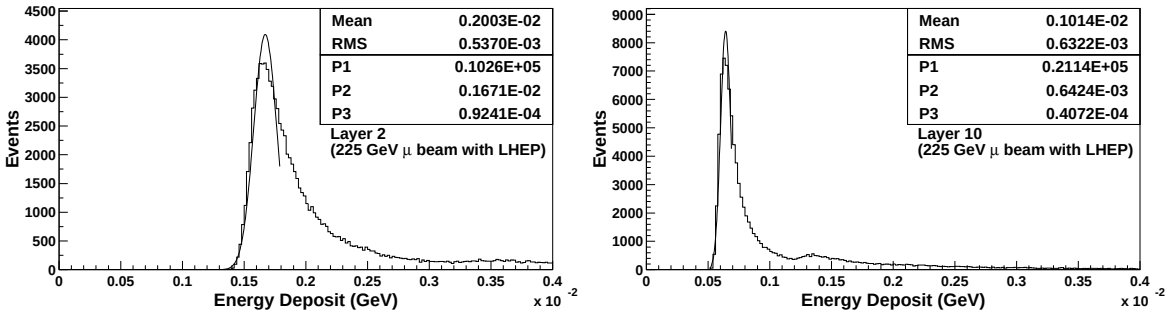

Figure 7: Muon energy deposit in layers 2, 10 using the physics list LHEP in GEANT4.

The simulated samples are likewise converted in terms of a MIP (Minimum Ionising Particle) signal using simulated muon beams of 225 GeV/c in the simulation. Figure 7 shows the energy distributions for layers 2 and 10 simulated with LHEP. Smooth lines are fits to a Gaussian near the peak region of the distribution.

4.2 Beam Background

Pion beams at high energies (above 50 GeV) had negligible background due to muons or electrons (less than 1% overall). At low energies there were substantial background due to muon (10% at 20 GeV and as high as 40% at 10 GeV). The electron contamination also increased from 3% at 30 GeV to 21% at 10 GeV. Stringent cuts have been applied to the data to remove the muon contamination below 1% at all energies. The largest conatmination

after cuts for pions at 10 GeV was due to electrons (estimated to be 5%). The same cuts are applied to data and Monte Carlo samples for all further comparisons.

Electron beams on the other hand had a sizable pion contamination at high energies ($\sim$ 25% at 150 GeV) which drops to less than 2% at lower energies. Contamination due to muons was 6% at 10 GeV and this dropped significantly at higher energies. The cuts reduced the muon contamination to negligible level at all energies and pion contamination at 150 GeV was reduced to less than 4%. Again the same cuts are applied to select good electron candidates from data and Monte Carlo samples.

4.3 Energy Measurement in HCAL

In runs with hadron calorimeter alone, the energy of a particle is constructed from the energy deposits in the individual layers of the calorimeter. The energy deposits are first converted to MIPs by dividing the energy in each layer by the energy deposit in that layer due to passage of a muon (using the muon runs). For experimental data, a muon run close in time to the pion run and taken with the same magnetic field is used. For simulated data, the conversion factor to MIPs is likewise determined for each setting of magnetic field. The number of MIPs is then weighed by the absorber thickness in front of the layer. Then the sum total of energy from all the layers is matched to the nominal beam energy to determine the HCAL energy scale factor. The 100 GeV pion beam is used for the calibration for data as well as Monte Carlo. Figure 8 shows the total energy distribution for 100 GeV pions.

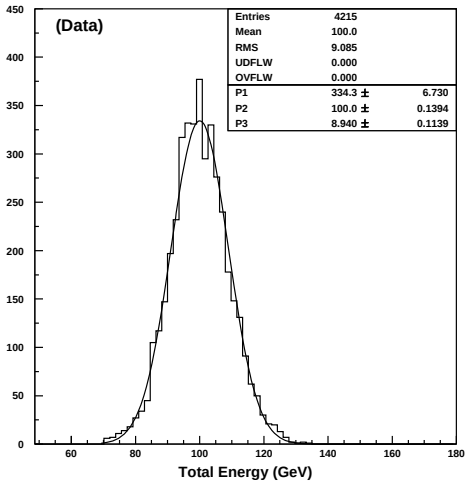

Figure 8: Energy distribution for 100 GeV pions in HCAL in the test beam data. The smooth curve is a fit to a Gaussian distribution.

4.4 Energy Measurement in ECAL

ECAL crystals were calibrated at the test beam using a 50 GeV electron beam. At first a normalisation is done using runs where the electron beam was pointing at the centre of each crystal. The peak of the energy distribution is fixed at the same value for all crystals. The overall energy scale is then determined from a run where the beam was pointing at the central crystal. Energies in the individual towers are added and the sum is compared with the nominal energy of the beam. For Monte Carlo sample, the relative calibration of the crystals is not carried out. Otherwise, the same procedure is followed. Figure 9 shows the energy distribution for 50 GeV electrons in ECAL from test beam data and from the QGSP model of GEANT4. A matrix of 5×5 towers surrounding the central crystal is found to contain the shower.

4.5 Energy Measurement in a Combined Setup

For a setup with both ECAL and HCAL, the energy of a particle is obtained from the sum of ECAL and HCAL energies. However, the scale factor for the hadron calorimeter is recomputed again using 100 GeV pion beam.

Energy distribution of pions, which start showering in ECAL, peaks at a lower value than the energy distribution of the ones which go through ECAL as minimum ionising particles. To a certain extent this can be taken care of by

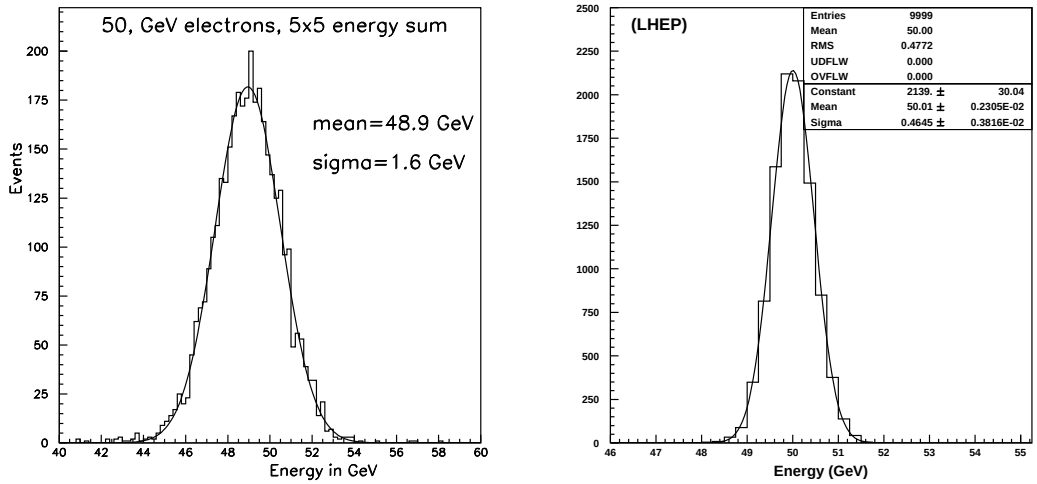

Figure 9: Energy distribution for a 50 GeV electron beam in HCAL: (a) Test beam 1996, (b) GEANT4 (LHEP).

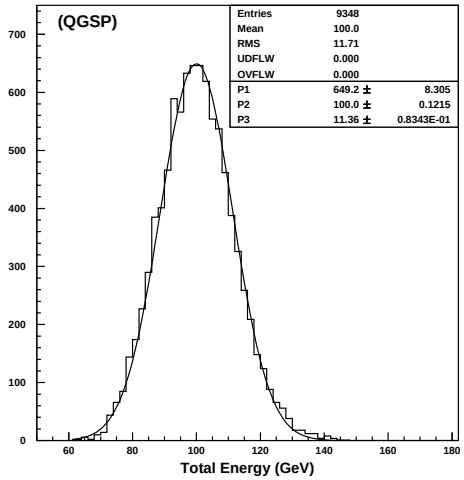

Figure 10: Energy distribution for 100 GeV pions in ECAL + HCAL in the simulated dataset generated using the QGSP physics list. The weighting technique is used to estimate the total energy. The smooth curve is a fit to a Gaussian distribution.

weighting the energy deposit in HCAL with respect to that in ECAL. Using different weights for different parts of HCAL works better than using a single weight for whole of HCAL. For this purpose the HCAL layers are divided into three different groups: first layer (H_1), layers 2 to 18 (H_2) and layers 19 to 28 (H_3). The total energy is given by equation 1.

$$\text{Total Energy} \quad = \quad E_{ECAL} + w_1 \cdot E_{H_1} + w_2 \cdot E_{H_2} + w_3 \cdot E_{H_3} \tag{1}$$

w_1, w_2 and w_3 are evaluated by minimising energy resolution for 100 GeV pions while constraining the mean value of the energy sum to the incident beam energy. Figure 10 shows the distribution of total energy for 100 GeV pions in the Monte Carlo sample generated using the QGSP physics list of GEANT4. One gets substantially better energy resolution than the default method (which does not use this weighting).

5 Studies with HCAL alone Setup

The HCAL system is studied with both pion and electron beams and also with different values of magnetic field. The various comparisons with Monte Carlo predictions are described below.

5.1 Pion Beam with no B-field

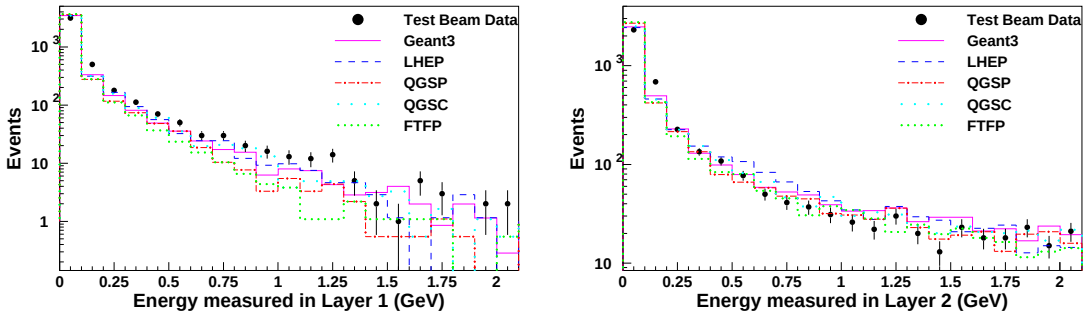

Figure 11: Energy deposit in HCAL layers 1 and 2.

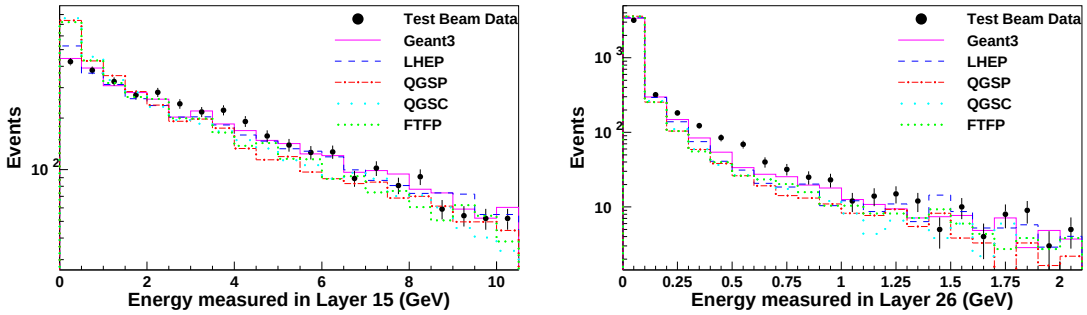

Figure 12: Energy deposit in HCAL layers 15 and 26.

Figures 11, and 12 show the distributions of energy deposited in HCAL layers 1, 2, 15 and 26 during the passage of a 100 GeV pion beam. There are no big differences between data and Monte Carlo, though some details are not exactly the same. For example, simulation shows an excess of events with low energy deposit in layer 15 which is not present in the data.

Figure 13 is a comparison of 100 GeV pion energy distribution as calculated from energy deposits in HCAL layers. The same plot also shows the ratio between Monte Carlo and data. The agreement is rather good for most of the GEANT4 models. However, GHEISHA provides somewhat broader distribution than the data. GEANT4 models seem to have a longer tail on the high energy side which is more prominent for LHEP and QGSC models. Table 1 summarises the RMS widths of these distributions. The calculated total energy has been fixed at 100 by the calibration procedure. Comparison of the measured widths shows the degree of agreement between data and Monte Carlo.

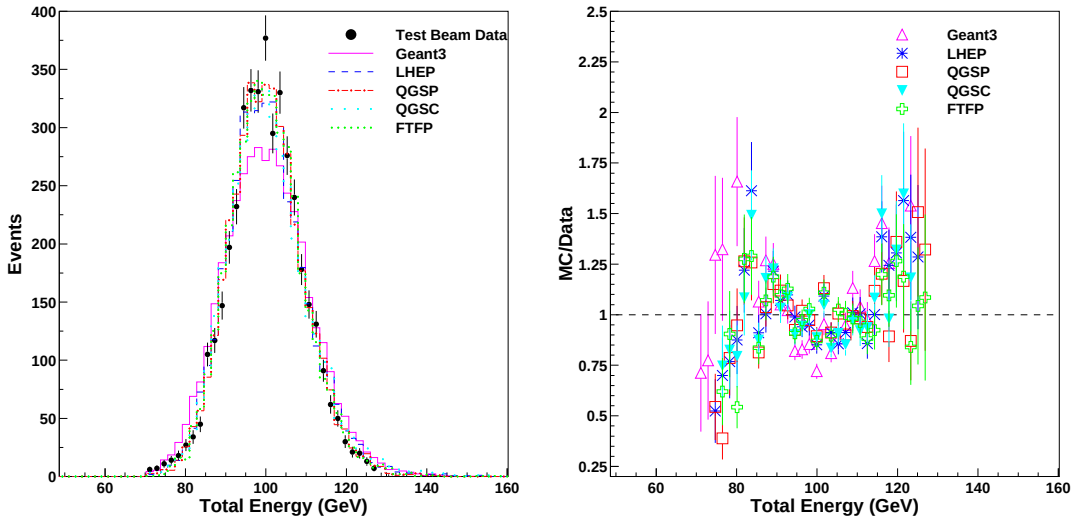

Figure 13: (a) Total energy measurement with 100 GeV pions in HCAL alone set up – the test beam data being compared with different Monte Carlo predictions. (b) The ratio of Monte Carlo to data for the total energy measurement.

	RMS (GeV)
Data	9.1±0.1
LHEP	9.9±0.1
QGSP	9.3±0.1
QGSC	10.7±0.1
FTFP	9.4±0.1
GHEISHA	10.8±0.1

Table 1: RMS values of energy distribution for 100 GeV pion beam in the HCAL alone setup. The mean is fixed at 100 GeV by the calibration procedure.

5.1.1 Energy Resolution and Response

Figures 14, 15 show energy distributions for pion beams in the HCAL alone setup with four different energies. Monte Carlo models show longer non-Gaussian tails than test beam data especially at lower beam energies.

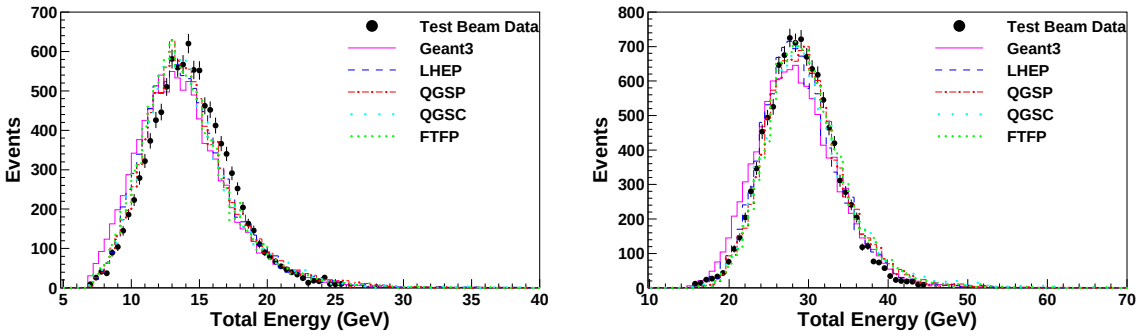

Figure 14: Comparison of total energy measurement between data and Monte Carlo in the HCAL alone setup with 15 and 30 GeV pions.

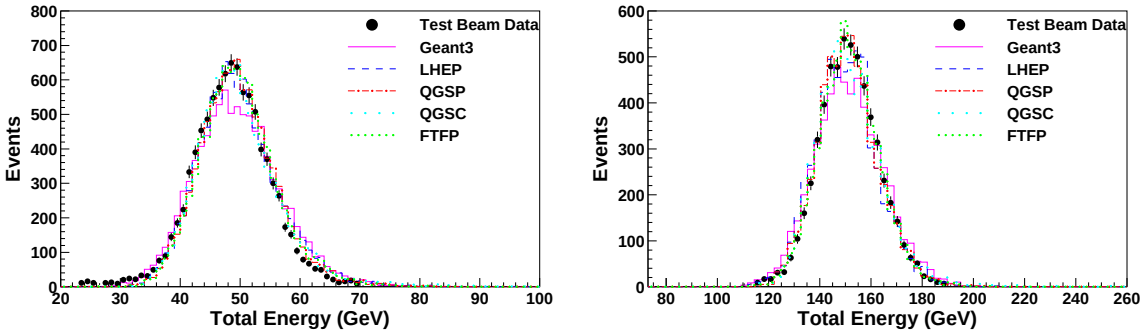

Figure 15: Comparison of total energy measurement between data and Monte Carlo in the HCAL alone setup with 50 and 150 GeV pions.

Since the energy distributions exhibit some non-Gaussian behaviour, mean and RMS of these distributions are used to determine the energy resolution. Figure 16 shows a plot of the energy resolution of the HCAL system for pions. At lower energies the resolution of the Monte Carlo samples is worse than that of test beam data. The ratio plot for resolution shows that QGSP and FTFP models are agreeing better than 5% with the data at beam energies above 50 GeV. The agreement worsens to 15% at lower beam energies.

Figure 17 shows the variation of energy response (ratio of measured to nominal energy) of the calorimeter to pions. One finds that the nonlinearity of the calorimeter increases with decreasing energy. The agreement between data and Monte Carlo models is rather good (better than 2% over a large energy region).

5.1.2 Longitudinal Shower Profile

Figure 18 shows the progress of longitudinal showers through HCAL for 100 GeV pion beam. The plot shows percentage of energy deposit as a function of layer number. As can be seen from the plot, the microscopic models of GEANT4 (QGSP, QGSC, FTFP) predict a more compact shower than the parametrised models (LHEP and GHEISHA). The data lie between the two models till layer 23 and at larger depths there is a better agreement with the parametrised models.

Figure 19 shows the propagation of a 150 GeV pion shower through HCAL. The same difference between microscopic and parametrised models is again observed. Data lie between the two set of expectations over a large range.

Figure 20 shows the variation of mean of the shower profile of pion beams in HCAL as a function of the beam energy. The mean of the shower profile distributions is seen to increase logarithmically with energy for data as well as with the Monte Carlo models. The agreement is better than 5% over the entire energy region for all the

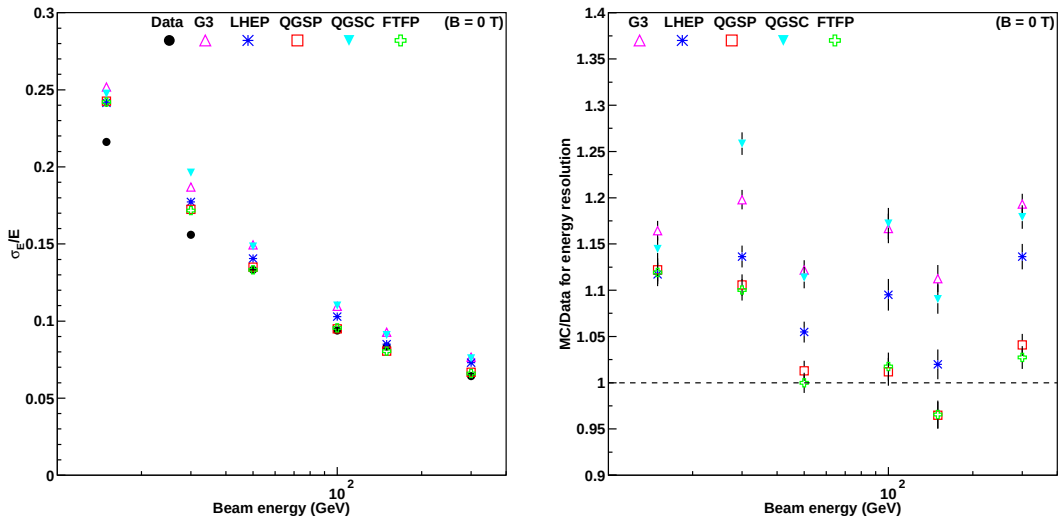

Figure 16: Variation of energy resolution with beam energy in the HCAL alone setup. The ratio of Monte Carlo to data is also shown.

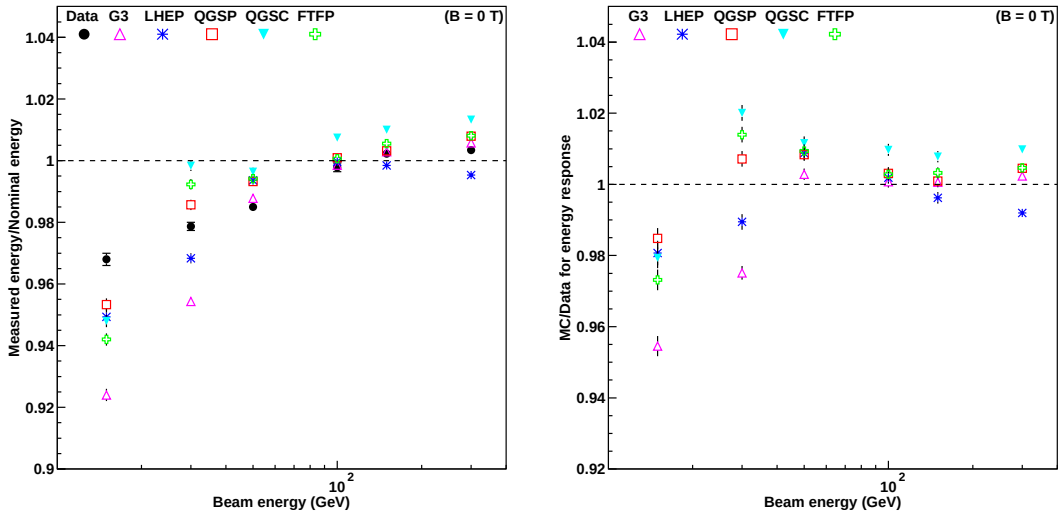

Figure 17: Variation of energy response with beam energy in the HCAL alone setup. The ratio of Monte Carlo to data is also shown.

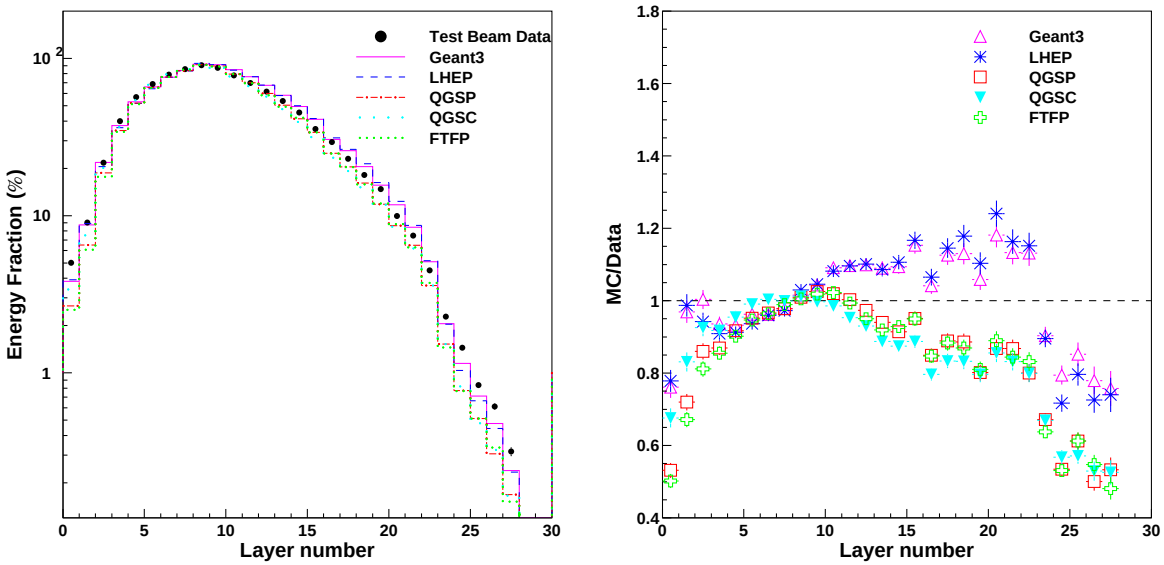

Figure 18: Longitudinal shower profile for 100 GeV pion beam in HCAL – test beam data being compared with predictions of different Monte Carlo models. The ratio of model prediction to data is also shown.

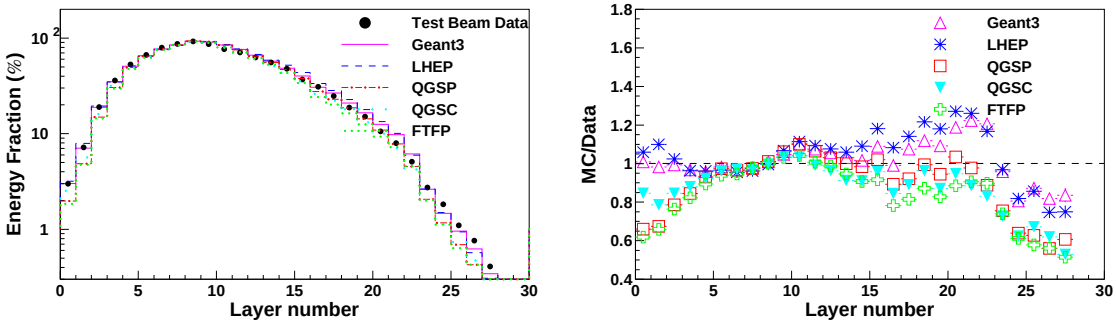

Figure 19: Longitudinal shower profile of 150 GeV pions in the HCAL alone setup.

models. The microscopic models of GEANT4 have agreements within 2%.

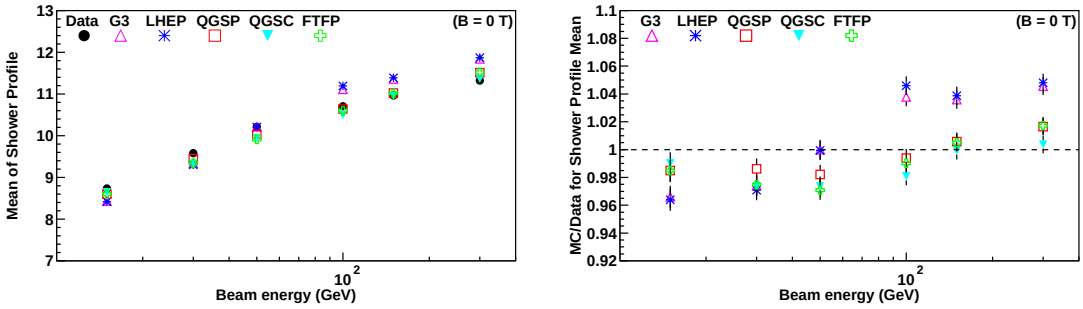

Figure 20: Comparison of the mean of the longitudinal shower profile distribution as a function of beam energy between data and different Monte Carlo models.

Figure 21 shows the variation of RMS spread of the shower profile distributions of pion beams in HCAL alone setup as a function of beam energy. The RMS also increases with energy in the data as well as in the Monte Carlo samples. All models provide good agreement with the data. Here, however, the agreement of the parametrised models (LHEP and GHEISHA) are significantly better at higher energies.

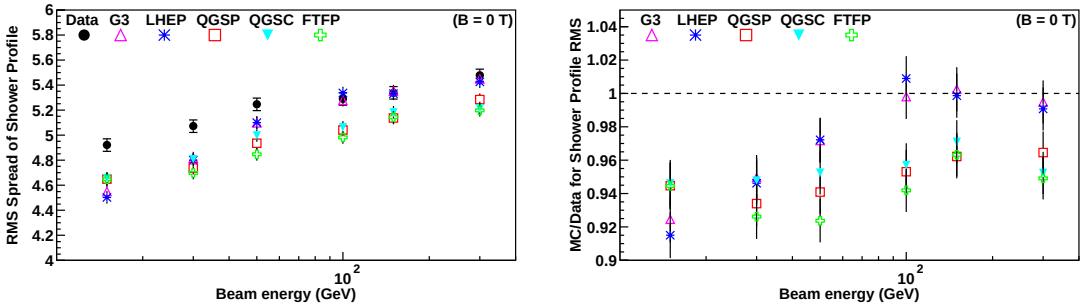

Figure 21: Comparison of RMS of the longitudinal shower profile distribution as a function of beam energy between data and different Monte Carlo models.

5.2 Electron Beam with no B-Field

Figure 22 shows the energy measured by HCAL of a 100 GeV electron beam. The energy of the electron has been calculated using the same scale factor which was used for the pion energy calculation. Since the response of HCAL to electrons is not the same as that to pions, the energy of the electron beam comes out to be quite different from 100 GeV. Table 2 lists values of mean and RMS of these energy distributions.

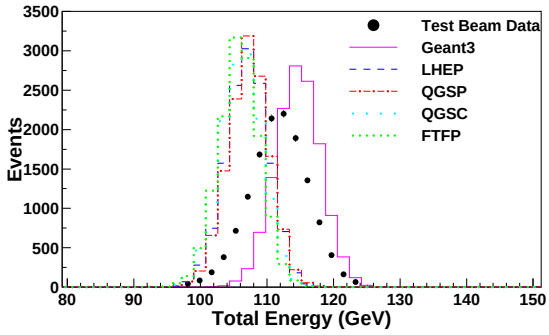

Figure 22: Total energy measurement for 100 GeV electron beam in HCAL.

Sample	Mean (GeV)	RMS (GeV)	RMS/Mean (%)
Data	111.8±0.03	4.71±0.03	4.21±0.03
LHEP	107.7±0.02	3.22±0.02	2.99±0.02
QGSP	108.1±0.03	3.23±0.02	2.99±0.02
QGSC	106.3±0.03	3.17±0.03	2.98±0.03
FTFP	106.9±0.03	3.19±0.02	2.98±0.02
GEANT3	115.3±0.03	3.48±0.02	3.02±0.02

Table 2: Comparison of energy distribution for Test Beam data and various models of GEANT4 and GEANT3 for 100 GeV electrons

5.2.1 e/h Ratio

The linearity of a calorimeter (variation of ratio of measured energy to beam energy with beam energy) and resolution depend on the intrinsic e/h, the ratio of the response to the electromagnetic and hadronic components in the shower. The average fraction of the electromagnetic component $F(\pi^0)$, in showers created by pions increases as a function of the incident energy. Using HCAL response to electrons and to pions, one can extract e/h, the ratio of electromagnetic to hadronic response according to the equations:

$$\pi = F(\pi^0) \times e + (1 - F(\pi^0)) \times h \tag{2}$$

$$\pi/e = (1 + (e/h - 1) \times F(\pi^0))/(e/h) \tag{3}$$

Figure 23 shows the electron to pion response ratio as a function of beam energy. As can be seen from the figure, all GEANT4 models predict a smaller value for the ratio over the entire energy region while GEANT3 predicts a larger value than the test beam data.

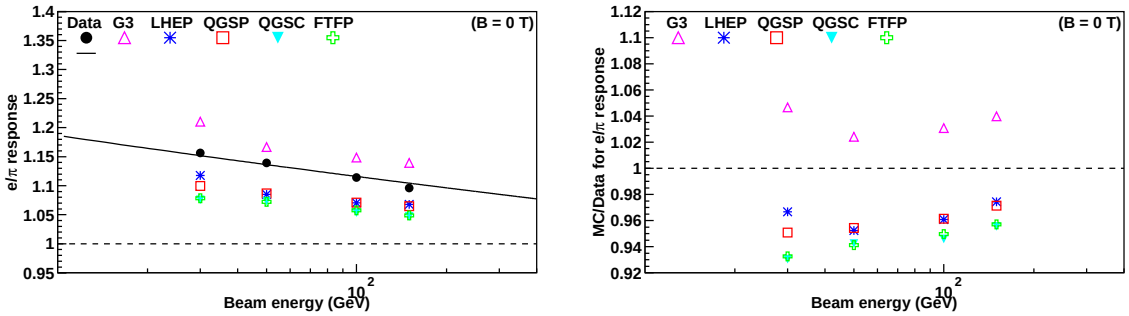

Figure 23: electron to pion ratio in HCAL.

The extracted value of e/h depends on the functional form assumed for $F(\pi^0)$ as a function of energy. The formulation due to Wigams [5] for $F(\pi^0)$:

$$F(\pi^0) = 0.11 \times \ln E \tag{4}$$

increases logarithmically with energy and becomes non-physical at very high energies. The subsequent parametrisation due to Gabriel *et al.* [6]:

$$F(\pi^0) = 1 - \left(\frac{E}{0.96}\right)^{-0.184} \tag{5}$$

takes care of saturation effect at very high energies. The values of e/h using these two different functional forms of $F(\pi^0)$ are given in Table 3. It can be concluded that the e/h ratio for HCAL is $\sim$ 3% higher in GEANT3 and 3-5% lower in the different models of GEANT4 than that in the test beam data.

	(Wigmans)	(Gabriel)
Data	1.27±0.06	1.33±0.07
LHEP	1.17±0.02	1.20±0.02
QGSP	1.16±0.01	1.19±0.02
QGSC	1.12±0.01	1.14±0.02
FTFP	1.13±0.01	1.15±0.02
GEANT3	1.36±0.02	1.44±0.02

Table 3: Values of e/h for two different functional forms of $F(\pi^0)$

5.2.2 Longitudinal Shower Profile

Figure 24 shows the shower profile for 100 GeV electron beam in HCAL. As can be seen from the plots the data show a somewhat broader distribution than the predictions of the MC models. One should keep in mind that the beam line is not described in the simulations. So the enhancement in layers 1 and 2 could be due to inadequacy of the geometry description. However, the longer tail in the data cannot be accounted for (unless effect of some beam background has not been properly taken into account).

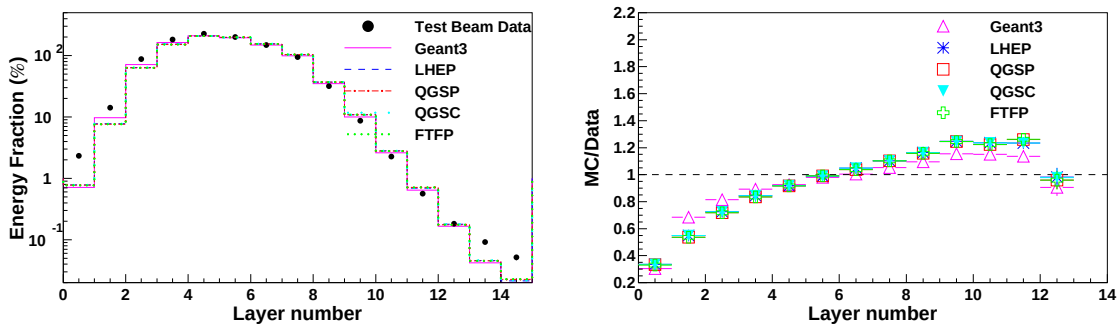

Figure 24: Longitudinal shower profile for 100 GeV electrons in HCAL being compared with predictions from several physics models of GEANT4 and GEANT3.

5.3 Pions in Presence of B-field

Data with pion beam are compared with predictions of several Monte Carlo models for the HCAL alone setup in the presence of the magnetic field.

5.3.1 Energy Response

Figures 25 shows the total energy measurement for 100 GeV pions with HCAL alone setup. The two plots show measurements at different magnetic field values: 0.0, 0.75, 1.5 and 3.0 Tesla. The peak position shifts towards higher values and the distribution gets broader as the field value is increased. This occurs both for test beam data and MC samples.

Tables 4 and 5 respectively show the peak and RMS values of total energy distributions for 100 GeV pion in HCAL alone setup at different settings of the magnetic field.

Figure 26 shows the mean energy response as a function of the B-field value for 100 GeV pion in hadron calorimeter. The increase in the measured energy with B-field, as seen in the data, is well explained by the Monte Carlo models.

Figure 27 shows energy resolution for 100 GeV pions in the hadron calorimeter as a function of B-field value. There is a slight increase in the energy resolution with magnetic field which is well reproduced by the Monte Carlo models.

5.3.2 Longitudinal Shower Profile

Figure 28 shows plots of energy deposits in HCAL layers 2, 8 and 14 for a 100 GeV pion beam. There are two sets of points and curves in these plots corresponding to field values of 0 and 3 Tesla. Broad features of simulated

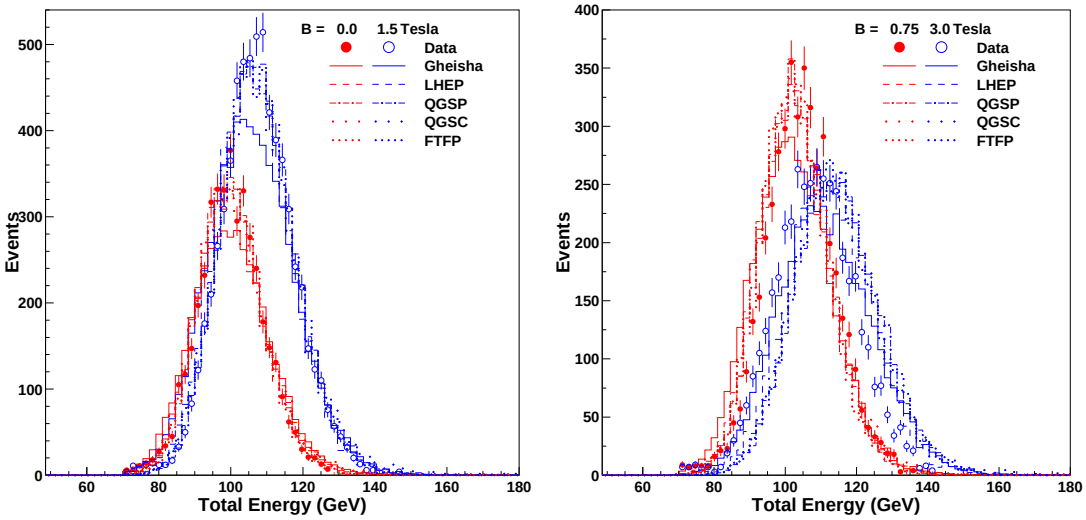

Figure 25: Total energy distribution for 100 GeV pions in HCAL alone setup for different settings of the magnetic field.

	Measured energy of 100 Gev π		
Sample	B = 0.75T	B = 1.50T	B = 3.00T
Data	103.4±0.1	106.7±0.1	108.4±0.2
LHEP	102.8±0.1	106.6±0.1	112.5±0.1
QGSP	103.0±0.1	107.5±0.1	114.6±0.1
QGSC	103.3±0.1	108.0±0.1	114.4±0.1
FTFP	102.8±0.1	107.7±0.1	114.1±0.1
GHEISHA	102.1±0.1	105.8±0.1	111.3±0.1

Table 4: Mean of total energy distributions of 100 GeV pions in HCAL at different settings of magnetic field for Test Beam data and various models of GEANT4 and GEANT3.

	RMS of E_{Total} for 100 Gev π		
Sample	B = 0.75T	B = 1.50T	B = 3.00T
Data	9.8±0.1	10.3±0.1	11.4±0.1
LHEP	10.4±0.1	10.9±0.1	11.9±0.1
QGSP	9.8±0.1	10.4±0.1	11.7±0.1
QGSC	11.0±0.1	11.7±0.1	12.7±0.1
FTFP	9.7±0.1	10.5±0.1	11.8±0.1
GHEISHA	11.1±0.1	11.9±0.1	13.2±0.1

Table 5: RMS of total energy distributions of 100 GeV pions in HCAL at different settings of magnetic field for Test Beam data and various models of GEANT4 and GEANT3.

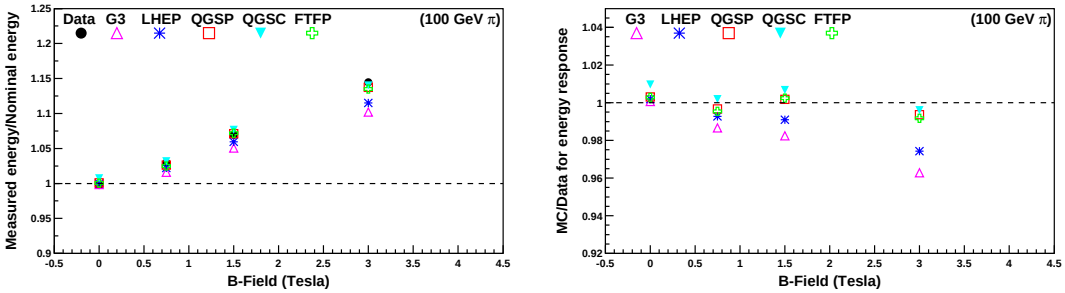

Figure 26: Energy response for 100 GeV pions at different field values for HCAL only.

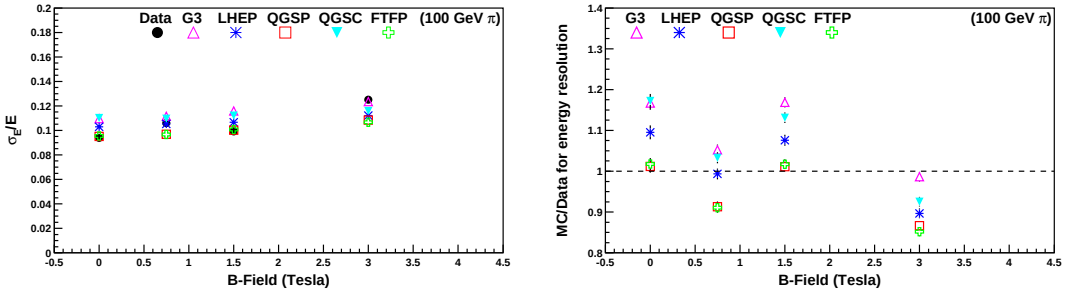

Figure 27: Energy resolution for 100 GeV pions at different field values for HCAL only.

samples look quite similar to those of test beam data. The comparison indicates that the increase in gain of the signal is maximum around the position of the shower peak. GEANT4 and GEANT3 models also show this effect. Similar to Figure 12 it is seen here that energy deposit is higher in both the early and later layers of HCAL in case of testbeam data.

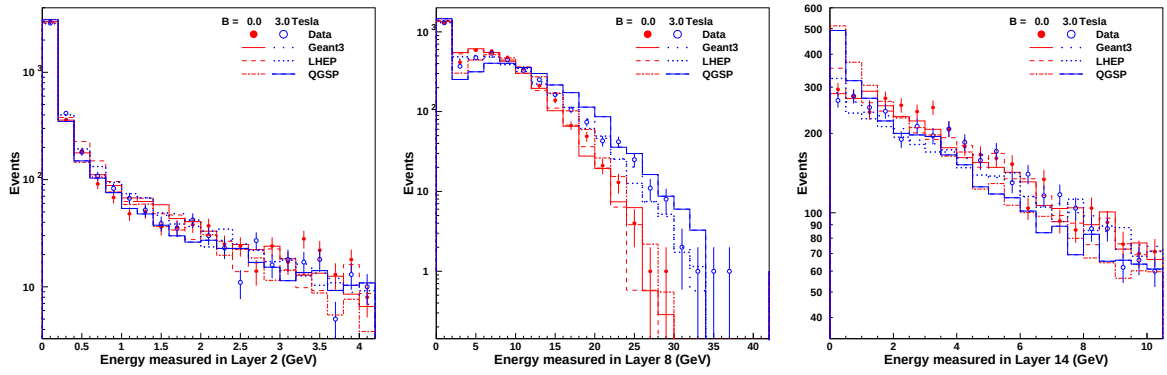

Figure 28: Distribution of measured energy for 100 GeV pion beams in HCAL layers 2, 8 and 14 in the HCAL alone setup with B-field values of 0 and 3 Tesla.

Figure 29 shows the variation of longitudinal shower profile of 100 GeV pions in the HCAL due to the presence of 1.5 and 3.0 Tesla magnetic fields. The shower profile for test beam data is broader than the Monte Carlo prediction and there is a clear indication that the increase in response is at the shower maximum.

5.4 Electrons in Presence of B-field

Data with electron beam are compared with predictions of several Monte Carlo models for the HCAL alone setup in the presence of the magnetic field.

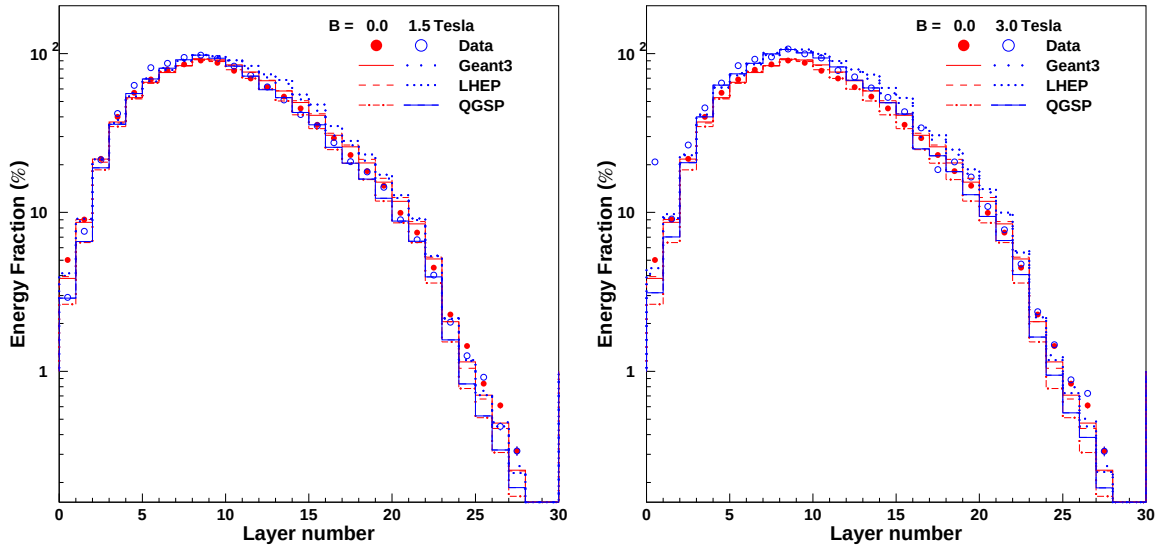

Figure 29: Longitudinal shower profile of 100 GeV pions in HCAL in presence of magnetic field of (a) 0.0 and 1.5 Tesla; (b) 0.0 and 3.0 Tesla.

5.4.1 Energy Response

Figures 30 shows the total energy measurement for 50 and 100 GeV electrons with HCAL alone setup. The two plots show measurements at two magnetic field values: 0.0 and 3.0 Tesla. The peak position shifts towards higher values and the distribution gets broader as the field value is increased for data as well as for Monte Carlo. The data show $\approx$ 19 % increase in the response for a B-field of 3.0 Tesla while the GEANT4 and GEANT3 models expect the increase to be 23% and 20% respectively.

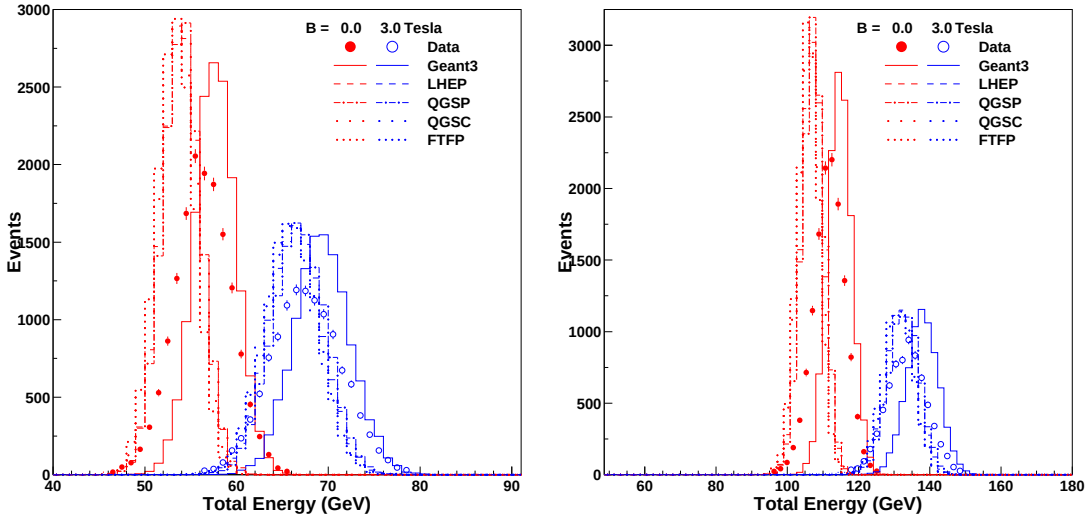

Figure 30: Total energy distribution for 50 GeV and 100 GeV electrons in HCAL alone setup for two settings of the magnetic field, 0 Tesla and 3.0 Tesla.

5.4.2 Longitudinal Shower Profile

Figure 31 shows the variation of longitudinal shower profile of 50 and 100 GeV electrons in the HCAL due to the presence of 3.0 Tesla magnetic field (compared with similar distributions with no B-field). The shower profiles show that there is a substantial increase in response near the shower maximum (layers 4–8) in the test beam data as well as in the Monte Carlo models.

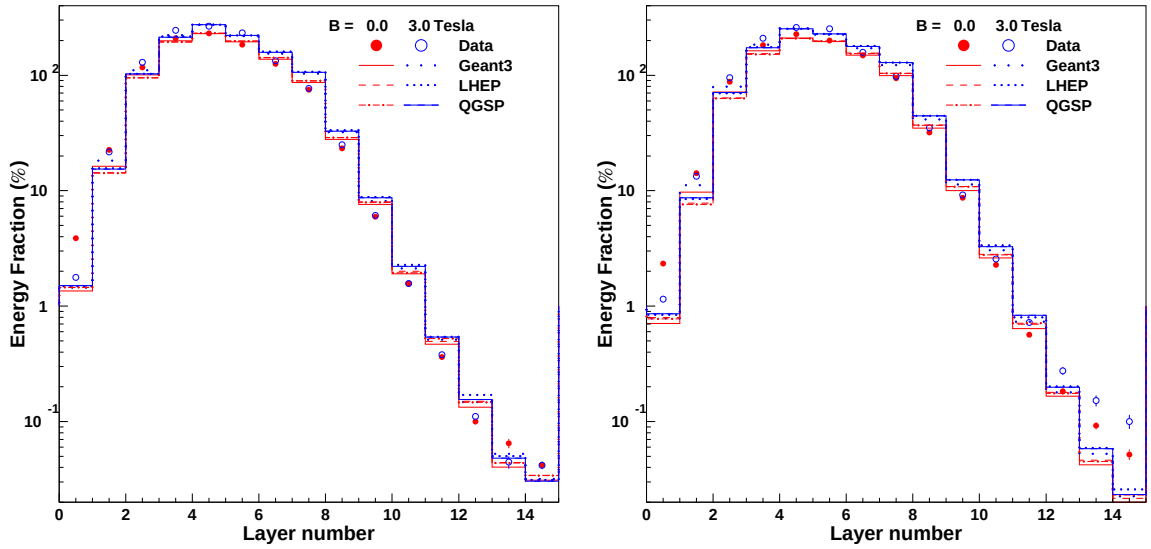

Figure 31: Longitudinal shower profile of 50 and 100 GeV electrons in HCAL in with (3.0 Tesla) and without magnetic field.

6 Studies with ECAL + HCAL System

Some of the pions, in a combined ECAL + HCAL setup, interact in the ECAL and start showering, while another set of pions sail through ECAL as minimum ionising particles and deposit their entire energy in HCAL. Figure 32 shows scatter plot for energy deposit in HCAL vs. energy deposit in ECAL for 100 GeV pions in test beam data and in the simulated sample with QGSP physics list. Data as well as Monte Carlo show some accumulation near zero ECAL energy (corresponding to MIP in ECAL) and a banana shape distribution (corresponding to shower starting in ECAL). The events which show small energy in both ECAL and HCAL are due to the small fraction of muons present in the pion beams.

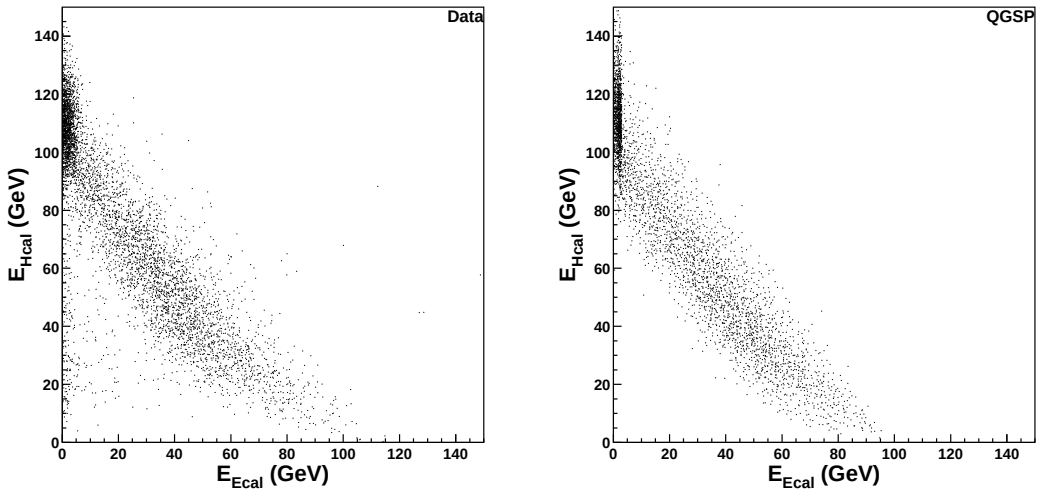

Figure 32: Energy deposit in HCAL versus energy deposit in ECAL for 100 GeV pions in ECAL + HCAL setup with no magnetic field in (a) test beam data, (b) simulated sample with QGSP.

6.1 Energy Response and Resolution

The energy resolution worsens if ECAL is present in front of HCAL due to the difference in e/h between ECAL and HCAL. Figure 33 shows the energy distribution of a 100 GeV pion beam going through ECAL and HCAL.

One sees that the energy distributions are somewhat broader for all MC models compared to the data. Table 6 gives the RMS values of the different distributions in the plot. The mean energy has been fixed at 100 GeV in the calibration procedure.

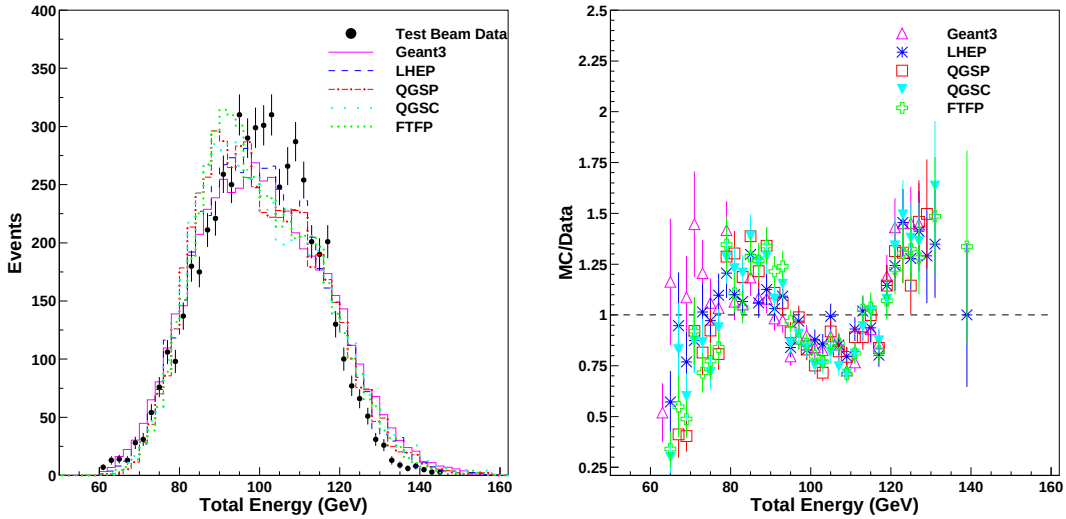

Figure 33: Comparison of total energy distribution for 100 GeV pions in ECAL + HCAL setup between data and various Monte Carlo models.

Sample	RMS (GeV)
Data	14.1±0.2
LHEP	15.0±0.1
QGSP	15.0±0.1
QGSC	16.1±0.1
FTFP	14.8±0.1
GHEISHA	16.0±0.2

Table 6: RMS values of total energy distribution for 100 GeV pions in ECAL + HCAL setup for the test beam data and various models of GEANT4 and GEANT3. The mean is fixed at 100 GeV by the calibration procedure.

A HCAL only situation can be simulated by taking the events where energy equivalent to a minimum ionizing particle is deposited in ECAL. This is done by selecting events which have less than 1 GeV energy in ECAL. Figure 34 show energy distributions for the two cases, MIPs in ECAL and shower in ECAL. Table 7 gives the mean and RMS values in these two cases.

	MIP in ECAL		Shower in ECAL	
Sample	Mean (GeV)	RMS (GeV)	Mean (GeV)	RMS (GeV)
Data	109.8±0.2	10.7±0.2	94.2±0.2	12.7±0.2
LHEP	111.7±0.2	12.0±0.2	92.7±0.1	11.7±0.1
QGSP	112.7±0.2	11.6±0.1	91.6±0.1	10.2±0.1
QGSC	113.1±0.2	12.8±0.2	92.2±0.1	12.0±0.1
FTFP	112.4±0.2	11.6±0.1	91.8±0.1	10.2±0.1
GHEISHA	113.0±0.2	12.6±0.1	92.5±0.1	12.4±0.1

Table 7: Comparison of energy distribution for 100 GeV pions in HCAL + ECAL between test beam data and various models of GEANT4 and GEANT3 when shower starts in HCAL or in ECAL.

The resolution for the total sample of events can be improved by bringing the two peaks closer to each other by reweighting the first layer of HCAL. The results after reweighting are shown in Figure 35 where the two samples (MIPs in ECAL and shower in ECAL) are separately shown and in Figure 36 where the combined sample is compared to the simulated samples. The energy resolution improves significantly and also the agreement between data and Monte Carlo becomes better. Table 8 gives the mean and RMS after reweighting. Table 9 gives the

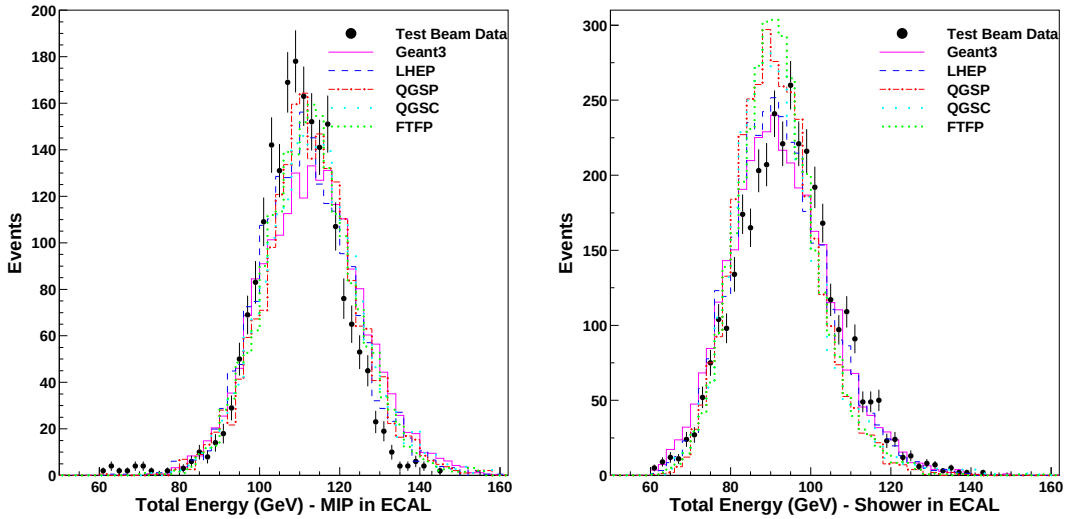

Figure 34: Comparison of total energy measurement for 100 GeV pions in ECAL + HCAL between test beam and different Monte Carlo models when (a) the pion is a minimum ionising particle in ECAL, (b) the shower starts in ECAL.

RMS values of the total sample (independent of the energy in ECAL). Comparison of the RMS values with those in Table 6 shows the improvement after reweighting.

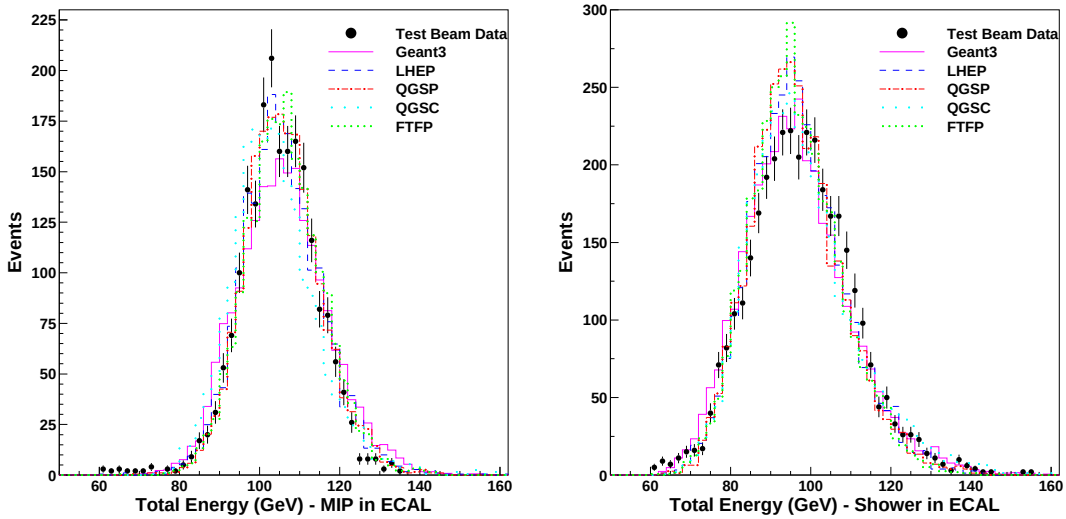

Figure 35: Comparison of total energy measurement of 100 GeV pions in ECAL + HCAL after reweighting the first HCAL layer between data and Monte Carlo when (a) there is a MIP in ECAL, (b) shower starts in ECAL.

Figure 37 shows the energy response curve (ratio of measured to nominal beam energy as a function of nominal beam energy) for the overall sample. All the GEANT4 models provide a very good description of the data. The nonlinearity at low energies is also explained within 5% (within systematic errors).

The nonlinearity effect is mainly due to the events which start showering in ECAL. Figures 38 and 39 show the response curves for the two sets of events, MIPs in ECAL and shower in ECAL respectively. The first set of plots is similar to the HCAL only configuration (with the exception that there is an overall shift of $\sim$ 10% in the measured energy which is an artefact of the calibration method, namely matching the mean of the overall sample to nominal beam energy at 100 GeV) and the agreement between data and Monte Carlo is well within 10%. The second set of plots shows that the deviation of measured energy from beam energy increases as energy increases upto $\sim$ 20-30 GeV and then it starts decreasing again. This decrease at the very low energies is not observed in simulated samples and the disagreement between data and Monte Carlo could be as high as 20%.

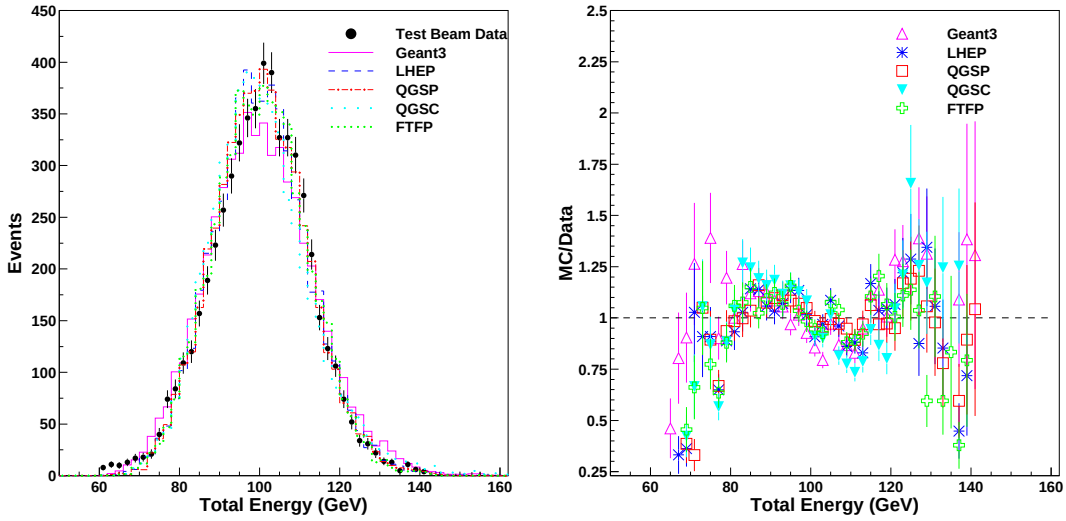

Figure 36: Comparison of total energy measurement of 100 GeV pions in ECAL + HCAL after reweighting the first HCAL layer between data and Monte Carlo.

	MIP in ECAL		Shower in ECAL	
Sample	Mean (GeV)	RMS (GeV)	Mean (GeV)	RMS (GeV)
Data	104.7±0.2	9.6±0.1	97.9±0.2	13.6±0.2
LHEP	105.7±0.2	10.2±0.1	96.8±0.2	11.7±0.1
QGSP	105.9±0.2	9.6±0.1	96.4±0.2	11.6±0.1
QGSC	104.0±0.2	11.3±0.1	97.9±0.2	13.8±0.1
FTFP	106.2±0.2	9.6±0.1	96.2±0.2	11.2±0.1
GHEISHA	105.9±0.1	11.2±0.1	96.7±0.1	13.3±0.1

Table 8: Mean and RMS of energy distribution for 100 GeV pions in ECAL + HCAL after reweighting in test beam data and various models of GEANT4 and GEANT3.

Sample	RMS (GeV)
Data	12.7 ± 0.2
LHEP	11.9 ± 0.1
QGSP	11.7 ± 0.1
QGSC	13.2 ± 0.1
FTFP	11.7 ± 0.1
GHEISHA	13.3 ± 0.1

Table 9: RMS of total energy distribution for 100 GeV pions in ECAL + HCAL after reweighting (all events). The mean is fixed at 100 GeV by the calibration procedure.

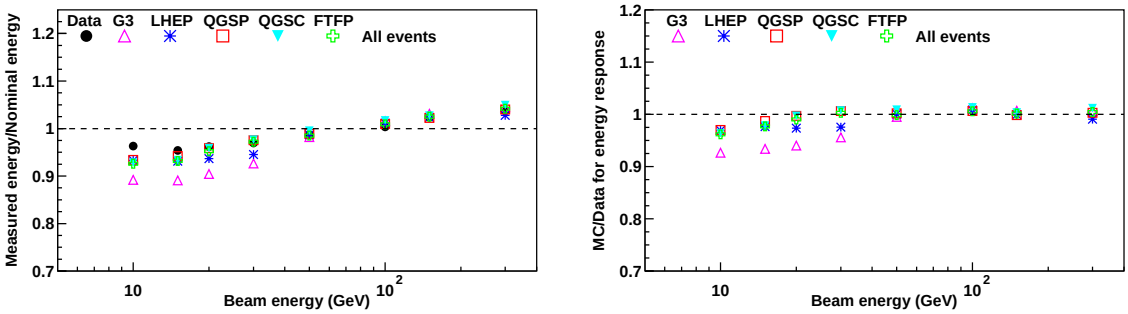

Figure 37: Comparison of energy response at different beam energies (all events) in the ECAL + HCAL setup.

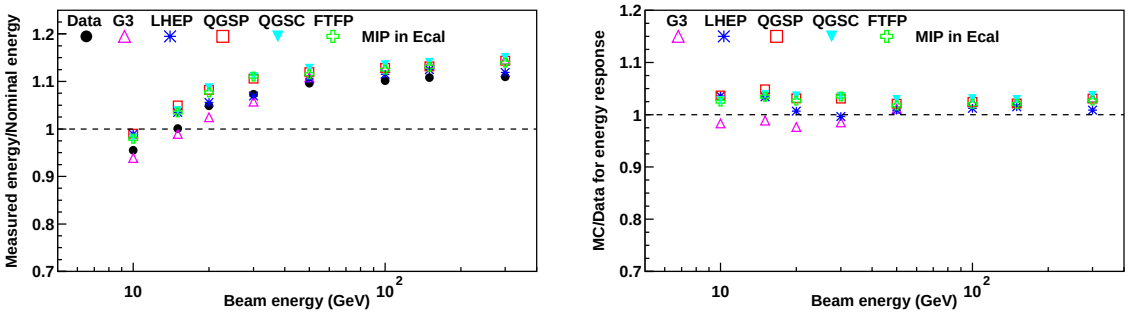

Figure 38: Comparison of energy response at different beam energies (MIP in ECAL) in the ECAL + HCAL setup.

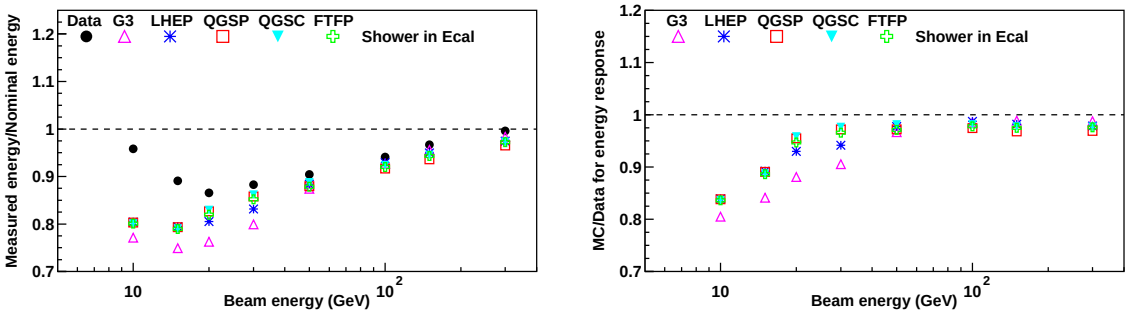

Figure 39: Comparison of energy response at different beam energies (Shower in ECAL) in the ECAL + HCAL setup.

Figure 40 shows the energy resolution (RMS/Mean of the total energy distribution) versus nominal beam energy. The energy resolution of test beam data is better than simulated data at energies below 20 GeV and becomes worse than simulated data by as much as 10-15% at high energies.

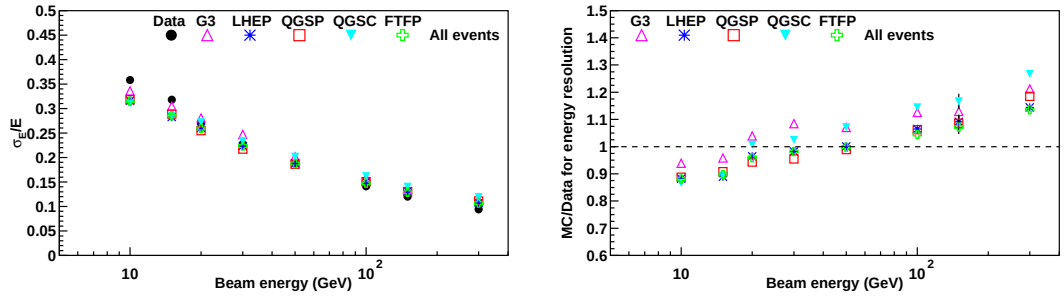

Figure 40: Comparison of energy resolution at different beam energies (overall sample) for pion beams in ECAL + HCAL setup.

Figure 41 shows the variation in energy resolution with pion beam energy in ECAL + HCAL system for events with MIPs in ECAL. Figure 42 shows the energy resolution for events with shower in ECAL. The agreement between data and some of the Monte Carlo models (like QGSP) is within 10% over the entire energy range in case the shower starts in HCAL. However in the sample where shower starts in ECAL, no model can provide reasonable agreement over the entire energy region. The level of disagreement at lower energies is as high as 20% or more.

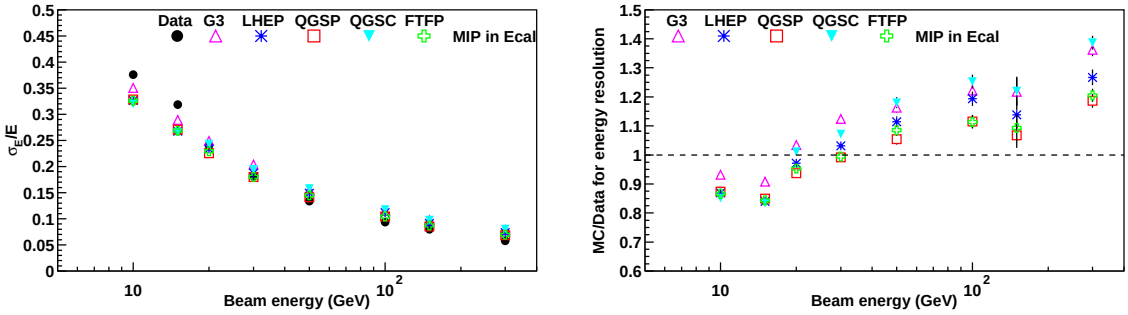

Figure 41: Comparison of energy resolution at different beam energies (MIPs in ECAL) for pion beams in ECAL + HCAL setup.

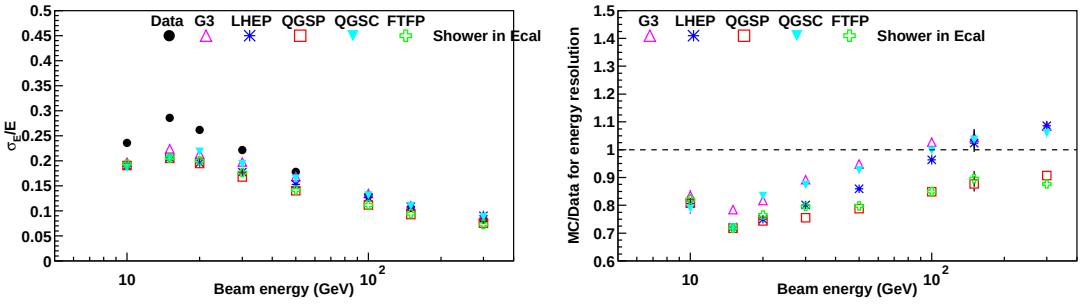

Figure 42: Comparison of energy resolution at different beam energies (Shower in ECAL) for pion beams in ECAL + HCAL setup.

6.2 Longitudinal Shower Profile

Figure 43 shows the logitudinal shower profile for 100 GeV pions. As seen in earlier profile plots, the profile for test beam data is wider than the simulation samples. The parametrised models with longer shower profiles are in better agreement with the data.

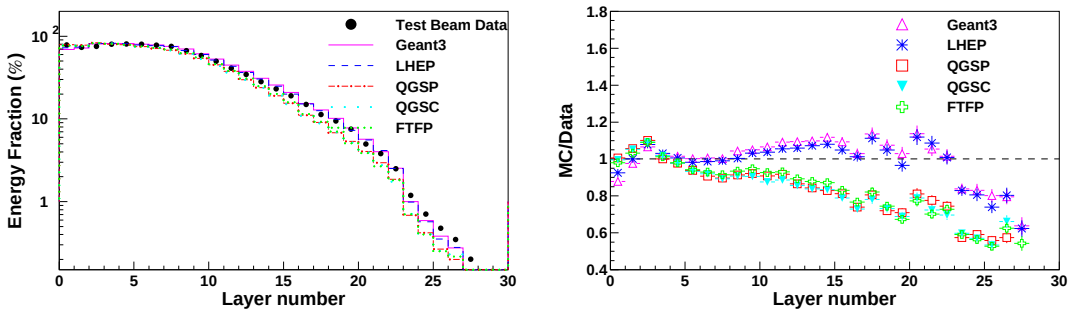

Figure 43: Longitudinal shower profile in HCAL of 100 GeV pion in ECAL + HCAL setup with the test beam data as well as with different Monte Carlo models.

Figure 44 shows a comparison of the mean values of the longitudinal shower profiles at different beam energies between test beam data and different Monte Carlo models. The data show an almost logarithmic dependence on energy which is also borne out by the Monte Carlo models. The agreement between data and Monte Carlo is within 5% and the parametrised models (LHEP and GEANT3) seem to have a better agreement at higher beam energies.

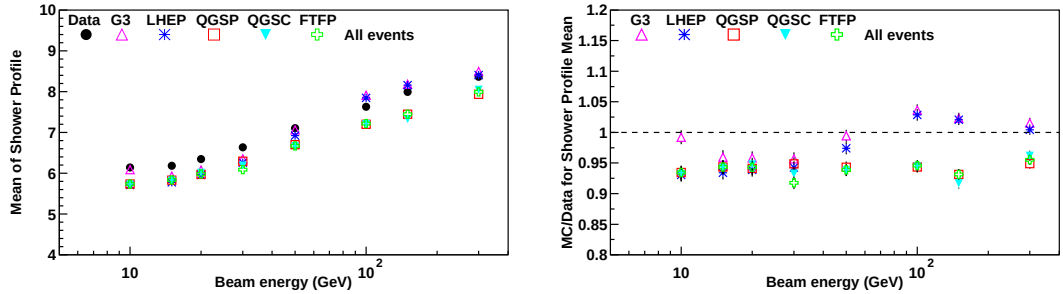

Figure 44: Comparison of mean of the longitudinal shower profiles at different beam energies with pion beams in ECAL + HCAL setup between test beam data and Monte Carlo models.

Figure 45 shows a comparison of the RMS spreads of the longitudinal shower profile at different beam energies. The RMS value decreases with increase in beam energy from 10 to 20 GeV and then it starts increasing with increase in beam energy almost following a logarithmic dependence. The Monte Carlo models, more particularly the parametrised models, follow the same trend and agree with data within 5%.

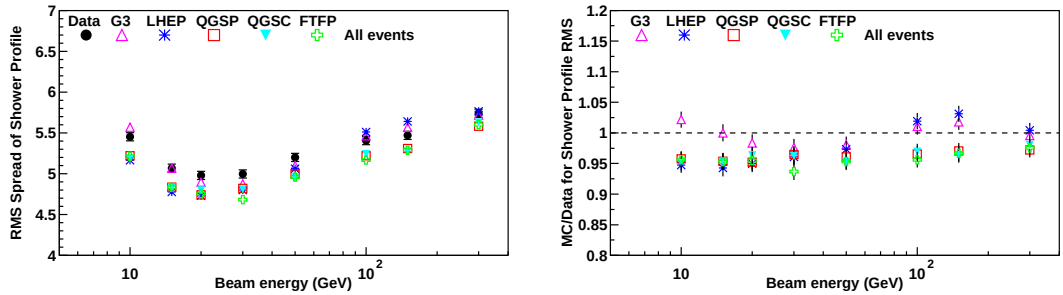

Figure 45: Comparison of RMS spread of the longitudinal shower profiles at different beam energies with pion beams in ECAL + HCAL setup between test beam data and Monte Carlo models.

7 Conclusions

The detailed comparison shown in the sections above helps us to pinpoint the regions of discrepancy in simulation of the physics of passage of particles through the hadron and electromagnetic calorimeters. Though gross features of the simulated samples look close to those in experimental data, there are many details which differ. Also, the different physics models of GEANT4 do not behave the same way.

Data collected during the test beam experiment are also influenced by the systematic effects due to beam background and electronic noise in the readout channels. Beam background is eliminated by using stringent selection criteria. Electronic noise is estimated from the data and is incorporated in the simulation.

The energy response of the calorimeters (HCAL standalone or ECAL and HCAL) to pion beam is well explained by the different models in GEANT4 over a wide energy region. Nonlinearity at lower beam energies are not so well reproduced by GEANT3.

Microscopic models like QGSP and FTFP explain energy resolution for pions in HCAL alone setup at high energies (above 50 GeV). The agreement worsens to 15% at lower beam energies. The other models in GEANT4 and GEANT3 provide worse agreement with the data. Energy resolution for pions in the combined setup has a worse agreement with the Monte Carlo models and the difference is higher than 20% for pions if the shower starts in ECAL.

The peak positions of longitudinal shower profiles for pions are better explained by the microscopic models of GEANT4 while the widths of the profile are in better agreement with the parametrised models (LHEP in GEANT4 and GEANT3).

e/π ratios in the data are within 5% of the model predictions and lie between the predictions of GEANT4 (which are lower) and GEANT3.

The enhancement in the response due to magnetic field is well reproduced by the models for pion as well as electron beams.

References

[1] The Compact Muon Solenoid (CMS) Technical Proposal, CERN/LHCC 94-38, December 5, 1994.

[2] See *http://geant4.web.cern.ch/geant4/*

[3] V. V. Abramov *et.al.*, Nucl. Instr. and Methods **A457** (2000) 75.

[4] R. Brun et al., *GEANT3 Users Guide.*, CERN Program Library W5013.

[5] R. Wigams $et\ al.$, Nucl. Instr. and Methods **A259** (1987) 389.

[6] T. A. Gabriel $et\ al.$, Nucl. Instr. and Methods **A338** (1994) 336.